The human counterpart of zebrafish *shiraz* shows sideroblastic-like microcytic anemia and iron overload

Clara Camaschella,[1,2] Alessandro Campanella,[1] Luigia De Falco,[4] Loredana Boschetto,[4] Roberta Merlini,[5] Laura Silvestri,[2] Sonia Levi,[1,2] and Achille Iolascon[3,4]

[1]Vita-Salute University and [2]Instituto di Ricerca e Cura a Carattere Scientifico (IRCCS) San Raffaele, Milan; [3]Department of Biochemistry and Medical Biotechnologies, University Federico II, Naples; [4]Centre of Genetics Engineering (CEINGE) Advanced Biotechnologies, Naples; [5]Department of Clinical and Biological Sciences, University of Turin, Turin, Italy

Inherited microcytic-hypochromic anemias in rodents and zebrafish suggest the existence of corresponding human disorders. The zebrafish mutant s*hiraz* has severe anemia and is embryonically lethal because of glutaredoxin 5 (*GRLX5*) deletion, insufficient biogenesis of mitochondrial iron-sulfur (Fe/S) clusters, and deregulated iron-regulatory protein 1 (IRP1) activity. This leads to stabilization of transferrin receptor 1 (*TfR*) RNA, repression of ferritin, and ALA-synthase 2 (*ALAS2*) translation with impaired heme synthesis. We report the first case of GLRX5 deficiency in a middle-aged anemic male with iron overload and a low number of ringed sideroblasts. Anemia was worsened by blood transfusions but partially reversed by iron chelation. The patient had a homozygous (c.294A>G) mutation that interferes with intron 1 splicing and drastically reduces *GLRX5* RNA. As in *shiraz,* aconitase and H-ferritin levels were low and TfR level was high in the patient's cells, compatible with increased IRP1 binding. Based on the biochemical and clinical phenotype, we hypothesize that IRP2, less degraded by low heme, contributes to the repression of the erythroblasts ferritin and ALAS2, increasing mitochondrial iron. Iron chelation, redistributing iron to the cytosol, might relieve IRP2 excess, improving heme synthesis and anemia. GLRX5 function is highly conserved, but at variance with zebrafish, its defect in humans leads to anemia and iron overload. (Blood. 2007;110:1353-1358)

Introduction

Hypochromic microcytic anemia results from deficiency of heme or globin synthesis in red cell precursors, as commonly occurs in iron deficiency and thalassemia and rarely in congenital sideroblastic anemias such as the X-linked form (XLSA), caused by mutations of the erythroid aminolevulinic acid synthase 2 (*ALAS2*),[1] and the variant associated with ataxia (XLSA/A), due to mutations of the mitochondrial iron-sulfur (Fe/S) cluster transporter *ABCB7*.

Animal models of other inherited microcytic anemias in rodents and zebrafish suggest the existence of corresponding human disorders. Recently a defective production of Fe/S clusters has been associated with deficient hemoglobin synthesis in *shiraz* zebrafish. In this pale mutant, blood cells are severely hypochromic, definitive hematopoiesis is defective, and the condition is lethal between day 7 and 10 after fertilization.[3] The *shiraz* phenotype is due to a large deletion encompassing the *GLRX5* gene,[3] which encodes a 156–amino acid mitochondrial enzyme belonging to an antioxidant protein family, highly conserved in eukaryotes. Studies in yeast have documented the essential role of GLRX5 in the synthesis of Fe/S clusters,[4] prosthetic groups that confer catalytic functions to several mitochondrial and cytosolic proteins involved in multiple metabolic pathways. The cytosolic iron-sensing IRP1, a key protein of iron metabolism, has constitutive RNA binding activity when devoid of Fe/S (apo-IRP1), while it acquires aconitase activity in the holo-form, associated with Fe/S cluster (Fe/S-IRP1).[5] IRP1 binds to iron responsive elements (IREs) in the 5′ or 3′ untranslated region of several target RNAs, which carry a functional IRE structure. The result of binding leads to transferrin receptor (*TfR*) transcript stabilization and *ferritin* and *ALAS2* translational repression, thus increasing iron uptake and decreasing its storage and utilization. Deletion of *GLRX5* in *shiraz* results in inhibition of aconitase activity, excessive IRP1 binding, and anemia because of ALAS2 inhibition.[3] The iron-sensing protein IRP2 has no role in *shiraz*[3]; however, being regulated by proteasomal degradation through iron and heme binding,[5] it has increased activity in a low-heme environment.

The early lethality of *shiraz* indicates that GLRX5 is essential for blood formation. Accordingly, *GLRX5* mRNA expression was found high in murine bone marrow, spleen, and liver.[3] No studies are available in humans, but human GLRX5 rescues the *shiraz* phenotype, suggesting that the enzyme is required for Fe/S cluster biosynthesis in vertebrates.[3]

Here we report the case of a middle-aged male with microcytic anemia due to a quantitative defect of *GLRX5*. The patient had moderate anemia, hepatosplenomegaly, low numbers of ringed sideroblasts, and iron overload. Surprisingly, anemia was worsened by blood transfusions but improved by iron chelation.

Patients, materials, and methods

The patient and controls gave informed consent in accordance with the Declaration of Helsinki for the study, which was approved by the

Submitted February 5, 2007; accepted April 25, 2007. Prepublished online as *Blood* First Edition paper, May 7, 2007; DOI 10.1182/blood-2007-02-072520.

An Inside *Blood* analysis of this article appears at the front of this issue.

The online version of this article contains a data supplement.

The publication costs of this article were defrayed in part by page charge payment. Therefore, and solely to indicate this fact, this article is hereby marked "advertisement" in accordance with 18 USC section 1734.

institutional review boards of the participating institutions. Molecular and cellular studies were performed 6 months after discontinuation of DFO.

Erythrocytes and peripheral blood mononuclear cells (PBMCs) were obtained by density gradient centrifugation in the proband and 3 controls (C_A, C_B, and C_C). Lymphoblastoid cell lines (LCLs) were prepared from the patient and 2 healthy volunteers (C1 and C2).

Case report

The patient, now a 64-year-old man, is the offspring of consanguineous (first cousins) parents from southern Italy. Besides mild anemia, personal history was unremarkable up to 44 years, when type 2 diabetes was diagnosed. The patient presented jaundice, dark skin, and liver and spleen enlargement (5 cm and 6 cm from the costal margin). Anemia (hemoglobin [Hb] level, 88.6 g/L) was microcytic with low reticulocyte count; high levels of transferrin saturation, serum ferritin, indirect bilirubin, and liver transaminases (Table 1); and decreased levels of haptoglobin and Hb A_2. Bone marrow showed moderate erythroid expansion and increased iron staining both in erythroblasts and macrophages, with 28% ringed sideroblasts. Folic acid and vitamin B_6 supplementation was ineffective.

At the age of 60 years, the patient first came to our attention because of severe anemia, which had required frequent packed red cell transfusions. Besides insulin-dependent diabetes, the patient had cirrhosis and hypogonadism. Hb level was 57 g/L with increased serum ferritin level and urinary iron excretion after deferoxamine (DFO) and elevated liver iron concentration (LIC; Table 1). Bone marrow biopsy, performed elsewhere, showed erythroid hyperplasia, abundant iron, and normal karyotype. Iron chelation was started with subcutaneous deferoxamine at 30 mg/kg with a portable pump for 10 hours daily. Clinical improvement was noticed within 6 months (Table 1). Serum ferritin level and LIC decreased, whereas Hb levels consensually increased until transfusions and iron chelation were stopped. Reevaluation of bone marrow revealed 12% ringed sideroblasts and 20% mitochondrial ferritin–positive erythroblasts.

Molecular studies

DNA was obtained from whole blood by standard methods. *GLRX5* exons and intron/exon boundaries were amplified by polymerase chain reaction (PCR) in the patient and healthy control DNA using specific primers (A1-A2, B1-B2, C1-C2 in Figure 1A; Table S1, available on the *Blood* website; see the Supplemental Materials link at the top of the online article). The amplified products were purified using the QIAamp purification kit (Qiagen, Valencia, CA) and sequenced by a fluorescent-tagged dideoxy chain terminator method in an ABI 310 automated sequencer (Applied Biosystems, Foster City, CA). The *GLRX5* cDNA from GenBank accession number NC_000014.7 was used as a reference sequence, where the A of the ATG translation initiation site represents nucleotide +1.

Total RNA was prepared from PBMCs or LCLs using the RNA extraction kit (PreAnalitix; Qiagen) and DNAseI (Invitrogen, Carlsbad, CA) to eliminate contaminating genomic DNA. Total RNA (2 μg) was reverse transcribed in a 20-μL reaction using Superscript III reverse transcriptase (Invitrogen). Primers D1-E2 were used to analyze *GLRX5* cDNA and primers D1-D2 and E1-E2 for exon-intron junction amplification (Figure 1A; Table S1). Fragments corresponding to exon-intron junctions were sequenced. Glucose 6-phosphate dehydrogenase (*G6PDH*) was used as control for amplification (expected fragment size for cDNA, 220 bp) and to exclude genomic contamination (expected size for genomic DNA, 1000 bp).

Quantitative real-time PCR

Quantitative real-time–PCR (qRT-PCR) was performed by SYBR Green PCR Master Mix (Applied Biosystems) by using Applied Biosystems Model 7900HT Sequence Detection System. Detailed methods and primer sequences are available on request. All PCR reactions were performed in triplicate. Relative gene expression was calculated by using the $2^{\Delta Ct}$ method, in which Ct indicates cycle threshold, the fractional cycle number where the fluorescent signal reaches the detection threshold.[6] The ΔCt was computed by calculating the difference of the average Ct between the

Table 1. Clinical and hematologic data of patients at diagnosis and during follow-up

Age, y	Hb level, g/L	MCV, fL	MCH level, pg	WBC count, × 10^9/L	Platelet count, × 10^9/L	Total bilirubin level, mg/dL	TF saturation, %	Ferritin level, mg/L	LIC, SQUID	Urinary iron level, mg/L	Red cell transfusions, units/mo	DFO, mg/kg/die
44	88.6	59	16	42	70	1.5	52	1100	—	—	—	—
56	70.0	51	15	33	105	1.1	—	1350	—	—	1–2	—
60	57.0	56	19	20	72	2.6	82	3124	3576	23.4	4–5	20 (7d/w)
61	70.2*	68	23	13	80	—	—	1547	2664	14	4	30 (6d/w)
62	97.0*	61	21	11	73	0.8	69	767	1823	15	3–4	30 (4d/w)
63	110*	66	22	28	79	1.27	—	1100	—	1.68	—	30 (4d/w)
64	113	64	22	28	73	0.92	43	664	900	0.8	—	—

Normal values were as follows: total bilirubin level, 0.2–1 mg/dL; TF saturation, <45%; ferritin level, <300 mg/L; LIC SQUID, <400 μg/g tissue wet/weight; and urinary iron level, <3 mg/L.

Hb indicates hemoglobin; MCV, mean corpuscular volume; MCH, mean corpuscular hemoglobin; WBC, white blood cell; TF, transferrin; LIC, liver iron concentration expressed in μg/g tissue wet/weight; SQUID, superconductum quantum interference device; DFO, subcutaneous deferoxamine; and —, not performed.

*Patient under transfusion regimen.

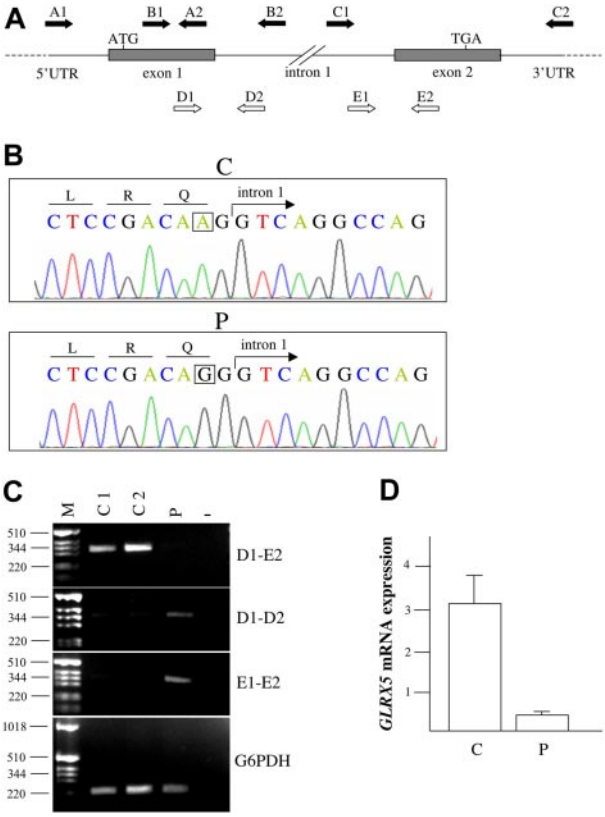

Figure 1. Genetic studies of the proband. (A) Schematic illustration of *GLRX5* gene. The arrows indicate primers used for genomic amplification (A1-A2, B1-B2, C1-C2), for semiquantitative determination of c*GLRX5* (D1-E2), and for exon-intron junction amplification (D1-D2, E1-E2) of proband and control cDNA. (B) Electropherograms of control (C) and proband (P) DNA in the region encompassing the exon 1–intron 1 boundary. The A→G homozygous mutation is boxed. (C) RT-PCR of *GLRX5* cDNA from P and controls (C1, C2) PBMC and a negative control (−). From top to bottom: The fragments corresponding to correctly spliced cDNA, obtained by using primers D1-E2, are reduced in the proband. The genomic regions encompassing exon1-intron1 (primers D1-D2) and intron1-exon2 (primers E1-E2) boundaries amplified on cDNA are significantly increased in the proband, suggesting a splicing defect. The identity of the fragments was verified by sequencing. G6PDH was used as control of the reverse transcription reaction and to demonstrate lack of genomic contamination. (D) Relative gene expression of *GLRX5* by qRT-PCR showing significant decrease in proband compared to controls. Error bars represent the standard error.

GLRX5 gene and the internal control *βactin.* The data are presented as mean ± the standard error (SE). The results were obtained on RNA samples prepared from 2 distinct PBMC samples.

Cell cultures

Cell culture media and reagents were from Invitrogen and Sigma-Aldrich (St Louis, MO). LCLs were maintained under standard conditions. When specified, LCLs were supplemented with 2 μM ^{55}FeAC (ferric ammonium citrate) for 18 hours.

Mitochondria isolation

Mitochondrial fractions (MFs) and postmitochondrial fractions (PMFs) of LCLs were separated by differential centrifugation and MFs were resuspended in an isotonic buffer as described.[7] For calculation of iron content, 10 μL of PMFs and MFs was resuspended in 0.3 mL of Ultima Gold scintillation liquid (PerkinElmer Life And Analytical Sciences, Wellesley, MA) and ^{55}Fe uptake was quantified in a beta counter. Counts per minute (cpm) were normalized on total protein content.

Western blot and immunoprecipitation

LCLs were lysed in 20 mM Tris-HCl (pH 7.4) supplemented with 0.05% Triton X-100 (for native Western blot [WB]) or 0.5% Triton X-100 (for denaturing WB and immunoprecipitation). Total protein content in soluble extracts was quantified by using the BCA method (Pierce, Rockford, IL). For TfR and β-actin determinations, 25 μg of soluble extracts was loaded onto a 10% denaturing sodium dodecyl sulfate–polyacrylamide gel electrophoresis (SDS-PAGE). Membranes were incubated with anti–β-actin (Sigma-Aldrich) and anti-TfR (Zymed Laboratories, San Francisco, CA) antibodies. For Apo- and Fe/S-IRP1 analysis, 10 μg of soluble extracts was separated by using a native 5% PAGE.[8]

Electro mobility shift assay (EMSA) was performed on 2 μg of soluble extracts using pSPT-Fer for IRE probe synthesis. Immunoprecipitation was performed on 500 μg of LCL soluble extracts using an anti-IRP2 antibody (courtesy of Paolo Arosio). Equal samples were loaded on 10% denaturing SDS-PAGE. After removal of nitrocellulose section corresponding to immunoglobulins, IRP2 was identified using the same antibody used for immunoprecipitation.

Enzymatic activities and ELISA

Aconitase and malate dehydrogenase (MDH) activities were assayed in mitochondrial and cytosolic LCL extracts, as described.[9] H ferritin was quantitated on PBMCs, LCLs, and erythrocytes by using enzyme-linked immunosorbent assay (ELISA).[10]

Results

Clinical and hematologic data

When first seen at 60 years of age, the patient appeared severely ill with a huge liver and spleen, severe anemia (and pancytopenia), iron overload with bronze diabetes, and cirrhosis. Blood transfusions had worsened the preexisting iron loading. In the differential diagnosis of microcytic anemia, we excluded (data not shown) both α- and β-thalassemia and DMT1 mutations (Mims et al,[11] Iolascon et al,[12] Beaumont et al[13]). Sideroblastic anemia was considered because of the presence of ringed sideroblasts, but the remarkable hepatosplenomegaly was not consistent with XLSA; XLSA with ataxia was ruled out by the absence of neurologic symptoms. An acquired clonal disorder was excluded by bone marrow studies. Finally, the fact that the patient had consanguineous parents strongly suggested a recessive condition.

Characterization of the *GLRX5* mutation

By sequencing *GLRX5* on the patient's genomic DNA, we identified a A→G homozygous transition at position 294 in the third nucleotide of the last codon of *GLRX5* exon 1 (Figure 1B). The CAA→CAG substitution does not change the encoded glutamine at position 98. However, since the change affects the penultimate nucleotide of exon 1, it is predicted to interfere with the correct RNA splicing.

In agreement with this hypothesis, amplification products of *GLRX5* cDNA from the patient's PBMCs were remarkably lower than in controls (Figure 1C left panel). Analysis of *GLRX5* expression by quantitative RT-PCR showed significantly decreased levels in the proband (mean 0.26 ± 0.03) compared with healthy subjects (mean 3.11 ± 0.41; $P < .01$ by 2-tailed t test; Figure 1C right panel). Compatible with a splicing defect, unspliced fragments encompassing the exon-intron junctions were easily amplifyable from the patient's cDNA (Figure 1C left panel).

Studies of iron homeostasis in the patient's cells

The analysis of iron proteins was carried out in the patient's LCLs and PBMCs, since no adequate erythroid material was available. To verify whether iron protein levels were consistent with cellular iron

status, iron incorporation was determined in both MFs and PMFs of LCLs supplemented with ferric ammonium citrate (FAC). Results obtained in the patient's LCLs (Figure 2) were compared with those of 2 controls, one with high (C1) and one with low (C2) iron incorporation. Cytosolic aconitase activity in the patient's LCLs, which showed high iron incorporation (Figure 2A), was lower than in controls (Figure 2B top panel), irrespective of their iron status (Figure 2A). Low aconitase activity in the patient's LCLs results from low levels of Fe/S-IRP1 protein, as shown by nondenaturing gel electrophoresis (Figure 2B bottom panel).[8] In addition, apo-IRP1 protein was low in the patient's LCLs, whereas it is typically increased in low-iron conditions, as in C2 (Figure 2B bottom panel).

As shown by EMSA, IRP1 was activated for binding activity in the patient's LCLs (Figure 2C top panel). IRP2 did not contribute to the signal, as assayed in supershift experiments by using a specific anti-IRP2 (not shown). We failed to identify IRP2 in Western blotting of LCL extracts, probably due to its low amount, as suggested by supershift experiments. To enrich the IRP2 protein, Western blotting was performed after immunoprecipitation of LCL extracts with the IRP2 antibody, exploiting the high molecular weight of IRP2 that allows separation from immunoglobulins. As expected from the levels of iron incorporation (Figure 2A), IRP2 was low in patient and C1 and high in C2 LCLs (Figure 2C bottom panel).

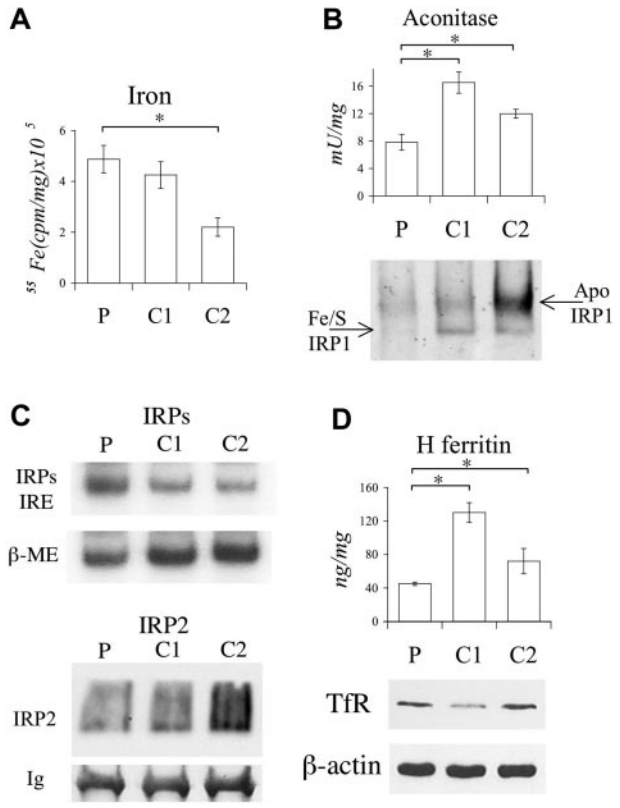

Figure 2. Functional studies on LCLs. (A) Cytosolic ^{55}Fe incorporation in proband (P) and 2 controls (C1 and C2). Cells were incubated with 2 μM ^{55}FeAC and after 18 hours cpm determined in postmitochondrial fractions (PMFs). (B; top) Cytosolic aconitase activity in P and controls. (Bottom) Determination of IRP1 conformation by immunoblotting of native PAGE. Separated Fe/S- and apo-IRP1 proteins are indicated by arrows. β-actin (shown in panel D) was used to confirm equal protein content. (C; top) IRE-IRPs electro mobility shift assay (EMSA). β-ME (beta-mercaptoethanol) was used to evaluate the total binding activity. (Bottom) Western blotting after immunoprecipitation of LCL extracts using anti-IRP2. Equal immunoprecipitation was verified by revealing immunoglobulins (Ig's). (D; top) H ferritin determined by specific ELISA. (Bottom) Western blotting of TfR. Equal loading was verified by β-actin. The experiments were repeated 3 times. Representative pictures are shown. Error bars represent standard deviations. *$P < .01$.

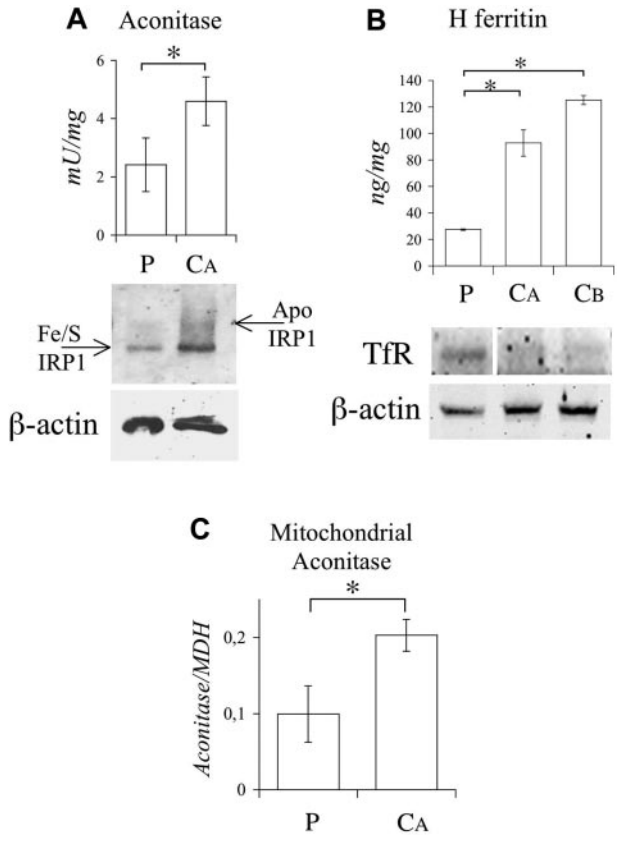

Figure 3. Functional studies on PBMCs. (A; top) Cytosolic aconitase activity in P and control. (Bottom) IRP1 conformation studies performed as described in Figure 2B. (B; top) H ferritin levels by ELISA. (Bottom) Western blotting of TfR. The vertical white line indicates a deleted lane in the same blot. Equal loading was verified by β-actin. (C) Mitochondrial aconitase activity as measured spectrophotometrically and normalized on mitochondrial malate dehydrogenase (MDH) activity. The experiments were repeated twice. Representative pictures are shown. Error bars represent standard deviations. *$P < .01$.

Consistent with the defective IRP1 sensing, in the patient's LCLs, H ferritin level was lower than in controls (Figure 2D top panel), whereas TfR was inappropriately high (Figure 2D bottom panel). The iron content in isolated MFs, after iron supplementation, paralleled that of PMFs (not shown).

The results obtained in LCLs were replicated in PBMCs. The patient's cytosolic aconitase activity was reduced (Figure 3A top panel) and Fe/S-IRP1 was low without increase of apo-IRP1 protein (Figure 3A bottom panel). The patient's H ferritin level was remarkably (70%–80%) lower (Figure 3B top panel) and TfR level higher (Figure 3B bottom panel) than in controls.

Our results demonstrate that, as in *shiraz,* mitochondrial GLRX5 deficiency affects cytoplasmic Fe/S-IRP1. The defect influences both PMF and MF compartments, as shown by reduction of mitochondrial (about 50%) aconitase in the patient's PBMCs (Figure 3C). However, a reduction of mitochondrial Fe/S cluster enzymes was not documented in LCLs, where the activity of aconitase and succinate dehydrogenase was normal. In addition, the patient's LCL protoporphyrin IX (PpIX), increased by ALA treatment, was decreased by iron addition (Figure S1), indirectly suggesting normal ferrochelatase activity.[14]

Red cell H ferritin level was remarkably high (3330 ± 270 ng/mg) in the patient compared with controls (696 ± 50 ng/mg).

Discussion

We have identified the human counterpart of zebrafish mutant *shiraz* in a patient with sideroblastic-like anemia and iron overload due to defective heme synthesis, secondary to IRP deregulation. In the patient's LCLs and PBMCs, we have shown that loss of GRLX5 activity converts IRP1 to a constitutive IRE-binding protein, as in *shiraz.* It is reasonable to postulate that in erythroid cells IRP1 binding activity represses ALAS2 translation and inhibits heme synthesis.[15] Heme deficiency and anemia are less severe in the human condition than in *shiraz,* reflecting the milder molecular defect (quantitative deficiency vs gene deletion). Indeed the patient clinical course was relatively benign, since a moderate anemia was recognized in midlife when the patient came to medical attention because of the onset of diabetes mellitus, a likely complication of iron overload. Surprisingly from that time onwards the Hb level progressively declined until the patient became transfusion dependent and anemia was partially reverted by iron chelation.

The human *GLRX5* defect provides unique insights into the mitochondrial-cytosolic iron homeostasis, unrecognized in *shiraz* because of its early lethality. The prevalent clinical expression as anemia is explained by the high heme requirement of erythroblasts coupled with the selective inactivation of *IRE-ALAS2*. Nonerythroid cells tolerate GLRX5 deficiency better than erythroid cells because of the lower requirement for heme and the presence of non–*IRE-ALAS1*. The absence of neurologic symptoms and signs of mitochondriopathies indicates that GLRX5 activity is indeed sufficient in cells other than the erythroid ones. The analysis of the iron phenotype of PBMCs and LCLs indicates that IRP1 is fully activated, ferritin level is low, and TfR level is high, suggesting that, as in *shiraz,* the low Fe/S cluster formation is sensed as a cytosolic iron deficiency. The patient's low IRP1 content might result from apoprotein degradation, which could contribute to control the effect of GLRX5 deficiency in PBMCs and LCLs.[16]

The degree of anemia was well tolerated, but iron overload was severe even before starting blood transfusions. In nonerythroid cells, where heme synthesis is presumably unaffected, deregulation of IRP1 by itself explains excessive iron uptake because IRP2 is degraded by high iron levels. On the contrary, in erythroid precursors where heme production is defective, IRP2 is expected to be less degraded. IRP2 does not rescue the phenotype in *shiraz,* where GLRX5 is fully lacking[3]; however, it has a prominent role in erythroid cells and its inactivation leads to deficient iron supply and anemia in *Irp2*$^{-/-}$ mice.[17,18] In addition, the IRP1 defect does not explain the severe phenotype observed at follow-up and the effect of iron chelation.

We hypothesize that IRP2 contributes to ALAS2 repression in the patient's erythroblasts, further decreasing heme synthesis and increasing mitochondrial iron (Figure 4), according to the view that the end product of the heme pathway regulates mitochondrial iron entry.[19] Hence, heme-defective cells with low cytosolic ferritin and high mitochondrial iron levels would undergo ineffective erythropoiesis, whereas erythrocytes with high cytosolic ferritin levels would gain the circulation. Since red cell ferritin level reflects erythroblast ferritin content,[20] high levels in the patient at follow-up may be the consequence of a preferential survival of erythroblasts with high cytosolic levels rather than mitochondrial iron levels. A role of IRP2 might also explain the paradoxical effect of iron chelation on anemia. DFO,[21] by shifting iron from mitochondria to the cytosolic compartment, might interrupt the vicious circle that up-regulates IRP2 (Figure 4), improving erythrocyte hemoglobinization and decreasing ringed sideroblasts.

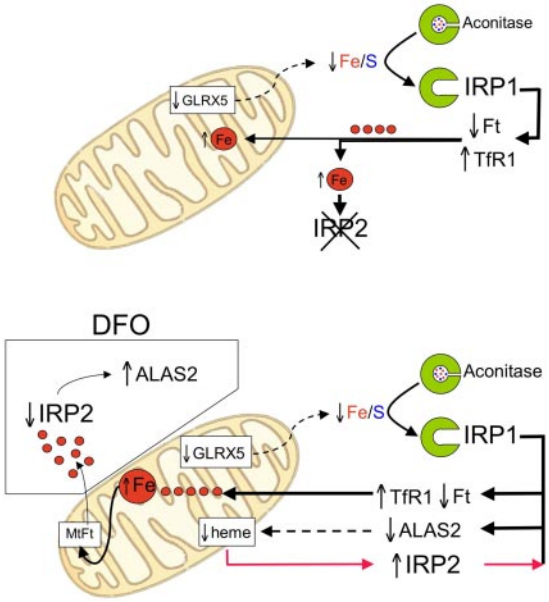

Figure 4. Model of iron and IRP regulation in GLRX5-deficient nonerythroid (top) and erythroid (bottom) cells. Mitochondria Fe/S cluster synthesis by GLRX5 and effect on cytosolic IRP1 and IRP2. ↑ and ↓ indicate increase or decrease, respectively. Small red circles are iron molecules. The arrows in bold indicate direction of movements, whereas dotted arrows indicate decreased effect. (Top) Impaired Fe/S cluster synthesis in nonerythroid cells activates cytosolic IRP1, leading to high cellular iron import. High iron levels degrade IRP2. Iron levels are increased at a similar extent both in the cytosol and the mitochondria. (Bottom) IRP1 activation occurs as in nonerythroid cells. Imported iron is directed to mitochondria, due to heme deficiency secondary to ALAS2 repression. Low heme allows high IRP2 activity, which potentiates the IRP1 effects (red arrows). This vicious circle may be relieved by DFO treatment (boxed on the left), which shifts iron to the cytosol, modulating IRP2 activity. See "Discussion" for details. GLRX5 indicates glutaredoxin-5; Ft, ferritin; TfR1, transferrin receptor; MtFt, mitochondrial ferritin; ALAS2, aminolevulinic-acid-synthase-2; and DFO, deferoxamine.

As an alternative hypothesis, we cannot exclude that the reactive oxygen species (ROS), produced by high iron levels, increase ineffective erythropoiesis and that iron chelation, by reducing ROS, ameliorates erythropoiesis and improves anemia.[22] Indeed GLRX5-deficient yeast, which lacks Fe/S enzyme activity and has mitochondrial iron overload, has increased ROS production.[23] However, ROSs were found normal in *shiraz.*[3]

The model illustrated in Figure 4 strengthens the role of IRPs in erythropoiesis and defines a link between the 2 mitochondrial pathways of iron utilization in erythroid cells, with Fe/S cluster regulating IRP1 and heme regulating IRP2. A mechanism based on this hypothesis could operate in congenital or acquired sideroblastic anemias, which show increased Hb levels after iron depletion.[1] Further studies on an erythroid model of GLRX5 deficiency are needed to explain the molecular basis of this phenomenon.

The human counterpart of *shiraz* confirms that GLRX5 function is highly conserved in vertebrates and links systemic iron homeostasis to mitochondrial iron utilization. The evidence that iron chelation ameliorates anemia, likely by partially restoring a physiologic iron sensing, suggests that manipulating the IRP unbalance might represent a therapeutic target in anemias with mitochondrial iron loading.

Acknowledgments

We are indebted to Rosangela Invernizzi for bone marrow Perls reaction and mitochondrial ferritin staining, to Antonio Piga and Filomena

Longo for SQUID evaluation, and to Cristina Scielzo for help in PpIX determination. We thank Paolo Arosio for helpful discussion.

This work was supported in part by Telethon Rome grant GGP05024 (C.C.) and GGP02202 (A.I.) and PRIN-MIUR Rome (C.C. and A.I.).

Authorship

Contribution: C.C. conceived the study, supervised the overall project, and drafted the paper. A.C., L.D.F., L.B., and L.S. performed research and helped to interpret the data. R.M. collected the samples and evaluated the patient. S.L. analyzed the data and helped to write the paper. A.I. supervised the research and contributed to writing the paper. All authors approved the final version of the manuscript.

Conflict-of-interest disclosure: The authors declare no competing financial interests.

Correspondence: Clara Camaschella, Università Vita-Salute San Raffaele, Via Olgettina, 60, 20132 Milano, Italy; e-mail: camaschella.clara@hsr.it.

References

1. Bottomley SS. Congenital sideroblastic anemias. Curr Hematol Rep. 2006;5:41-49.
2. Bekri S, Kispal G, Lange H, et al. Human ABC7 transporter: gene structure and mutation causing X-linked sideroblastic anemia with ataxia with disruption of cytosolic iron-sulfur protein maturation. Blood. 2000;96:3256-3264.
3. Wingert RA, Galloway JL, Barut B, et al. Deficiency of glutaredoxin 5 reveals Fe-S clusters are required for vertebrate haem synthesis. Nature. 2005;436:1035-1039.
4. Rodriguez-Manzaneque MT, Tamarit J, Belli G, Ros J, Herrero E. Grx5 is a mitochondrial glutaredoxin required for the activity of iron/sulfur enzymes. Mol Biol Cell. 2002;13:1109-1121.
5. Hentze MW, Kuhn LC. Molecular control of vertebrate iron metabolism: mRNA-based regulatory circuits operated by iron, nitric oxide, and oxidative stress. Proc Natl Acad Sci U S A. 1996;93:8175-8182.
6. Livak KJ, Schmittgen TD. Analysis of relative gene expression data using real-time quantitative PCR and the 2(-Delta Delta C(T)) Method. Methods. 2001;25:402-408.
7. Corsi B, Cozzi A, Arosio P, et al. Human mitochondrial ferritin expressed in HeLa cells incorporates iron and affects cellular iron metabolism. J Biol Chem. 2002;277:22430-22437.
8. Campanella A, Levi S, Cairo G, Biasiotto G, Arosio P. Blotting analysis of native IRP1: a novel approach to distinguish the different forms of IRP1 in cells and tissues. Biochemistry. 2004;43:195-204.
9. Campanella A, Isaya G, O'Neill HA, et al. The expression of human mitochondrial ferritin rescues respiratory function in frataxin-deficient yeast. Hum Mol Genet. 2004;13:2279-2288.
10. Cozzi A, Levi S, Bazzigaluppi E, Ruggeri G, Arosio P. Development of an immunoassay for all human isoferritins, and its application to serum ferritin evaluation. Clin Chim Acta. 1989;184:197-206.
11. Mims MP, Guan Y, Pospisilova D, et al. Identification of a human mutation of DMT1 in a patient with microcytic anemia and iron overload. Blood. 2005;105:1337-1342.
12. Iolascon A, d'Apolito M, Servedio V, Cimmino F, Piga A, Camaschella C. Microcytic anemia and hepatic iron overload in a child with compound heterozygous mutations in DMT1 (SCL11A2). Blood. 2006;107:349-354.
13. Beaumont C, Delaunay J, Hetet G, Grandchamp B, de Montalembert M, Tchernia G. Two new human DMT1 gene mutations in a patient with microcytic anemia, low ferritinemia, and liver iron overload. Blood. 2006;107:4168-4170.
14. Luksiene Z, Eggen I, Moan J, Nesland JM, Peng Q. Evaluation of protoporphyrin IX production, phototoxicity and cell death pathway induced by hexylester of 5-aminolevulinic acid in Reh and HPB-ALL cells. Cancer Lett. 2001;169:33-39.
15. Rouault TA. Linking physiological functions of iron. Nat Chem Biol. 2005;1:193-194.
16. Clarke SL, Vasanthakumar A, Anderson SA, et al. Iron-responsive degradation of iron-regulatory protein 1 does not require the Fe-S cluster. EMBO J. 2006;25:544-553.
17. Galy B, Ferring D, Minana B, et al. Altered body iron distribution and microcytosis in mice deficient in iron regulatory protein 2 (IRP2). Blood. 2005;106:2580-2589.
18. Cooperman SS, Meyron-Holtz EG, Olivierre-Wilson H, Ghosh MC, McConnell JP, Rouault TA. Microcytic anemia, erythropoietic protoporphyria, and neurodegeneration in mice with targeted deletion of iron-regulatory protein 2. Blood. 2005;106:1084-1091.
19. Ponka P. Tissue-specific regulation of iron metabolism and heme synthesis: distinct control mechanisms in erythroid cells. Blood. 1997;89:1-25.
20. Cazzola M, Dezza L, Bergamaschi G, et al. Biologic and clinical significance of red cell ferritin. Blood. 1983;62:1078-1087.
21. Hershko C, Link G, Konijn AM, Huerta M, Rosenmann E, Reinus C. The iron-loaded gerbil model revisited: effects of deferoxamine and deferiprone treatment. J Lab Clin Med. 2002;139:50-58.
22. Vreugdenhil G, Smeets M, Feelders RA, van Eijk HG. Iron chelators may enhance erythropoiesis by increasing iron delivery to haematopoietic tissue and erythropoietin response in iron-loading anaemia. Acta Haematol. 1993;89:57-60.
23. Rodriguez-Manzaneque MT, Ros J, Cabiscol E, Sorribas A, Herrero E. Grx5 glutaredoxin plays a central role in protection against protein oxidative damage in Saccharomyces cerevisiae. Mol Cell Biol. 1999;19:8180-8190.